The nuclear RNase III Drosha initiates microRNA processing

Yoontae Lee[1], Chiyoung Ahn[1], Jinju Han[1], Hyounjeong Choi[1], Jaekwang Kim[1], Jeongbin Yim[1], Junho Lee[2], Patrick Provost[3], Olof Rådmark[4], Sunyoung Kim[1] & V. Narry Kim[1]

[1]*Institute of Molecular Biology and Genetics and School of Biological Sciences, Seoul National University, Seoul 151-742, Korea*
[2]*Department of Biology, Yonsei University, Seoul 120-749, Korea*
[3]*Centre de Recherche en Rhumatologie et Immunologie, Centre de Recherche du CHUL, Ste-Foy, Quebec, Canada G1V 4G2*
[4]*Department of Medical Biochemistry and Biophysics, Karolinska Institute, Stockholm S-171 77, Sweden*

Hundreds of small RNAs of ~22 nucleotides, collectively named microRNAs (miRNAs), have been discovered recently in animals and plants[1–10]. Although their functions are being unravelled[1,2,11–13], their mechanism of biogenesis remains poorly understood. miRNAs are transcribed as long primary transcripts (pri-miRNAs) whose maturation occurs through sequential processing events: the nuclear processing of the pri-miRNAs into stem-loop precursors of ~70 nucleotides (pre-miRNAs), and the cytoplasmic processing of pre-miRNAs into mature miRNAs[14]. Dicer, a member of the RNase III superfamily of bidentate nucleases, mediates the latter step[15–19], whereas the processing enzyme for the former step is unknown. Here we identify another RNase III, human Drosha, as the core nuclease that executes the initiation step of miRNA processing in the nucleus. Immunopurified Drosha cleaved pri-miRNA to release pre-miRNA *in vitro*. Furthermore, RNA interference of Drosha resulted in the strong accumulation of pri-miRNA and the reduction of pre-miRNA and mature miRNA *in vivo*. Thus, the two RNase III proteins, Drosha and Dicer, may collaborate in the stepwise processing of miRNAs, and have key roles in miRNA-mediated gene regulation in processes such as development and differentiation.

We have previously shown that miRNA genes are expressed as primary transcripts (pri-miRNAs) that are longer than pre-miRNAs[14]. Pri-miRNAs are trimmed into ~70-nucleotide (nt) pre-miRNA forms, mainly in the nucleus[14,20]. After this initial processing, the pre-miRNAs are exported to the cytoplasm, and are cleaved to generate the final products of ~22 nt by Dicer[15–19]. Although Dicer-mediated processing has been studied intensively, the initiation step remains uncharacterized.

To understand the mechanism of the initial processing, we first determined the sites of cleavage by mapping the 5′ and 3′ ends of pre-miRNA. Pre-miR-30a was cloned by the directional cloning method originally described by Tuschl and others[21]. Briefly, pre-miR-30a was prepared by *in vitro* processing of pri-miRNA labelled with low specific activity and ligated to 5′ and 3′ adaptor molecules, followed by RT–PCR (polymerase chain reaction with reverse transcription), cloning and sequencing (Supplementary Information). The result showed that pre-miR-30a is a stem-loop of 63 nt (Fig. 1a). Interestingly, the stem-loop contains a 2-nt overhang at its 3′ end, which is a characteristic of the products of the RNase-III-mediated cleavage reaction. It is also intriguing that the termini of pre-miR-30a are identical to those of mature miR-30a and miR-30a*, indicating that the initial processing may predetermine the sequences of the final products.

To further characterize the nuclease activity towards pri-miRNA, *cis*-acting requirements for processing were examined by a series of mutations on miR-30a. Deletional mutagenesis followed by *in vitro* processing showed that the sequences covering 20 nt upstream and 25 nt downstream from the cleavage sites are sufficient to support processing (Fig. 1a and Supplementary Information), indicating that the *cis*-acting elements reside in the immediate vicinity and/or inside stem-loop pre-miRNA. Site-directed mutagenesis was then

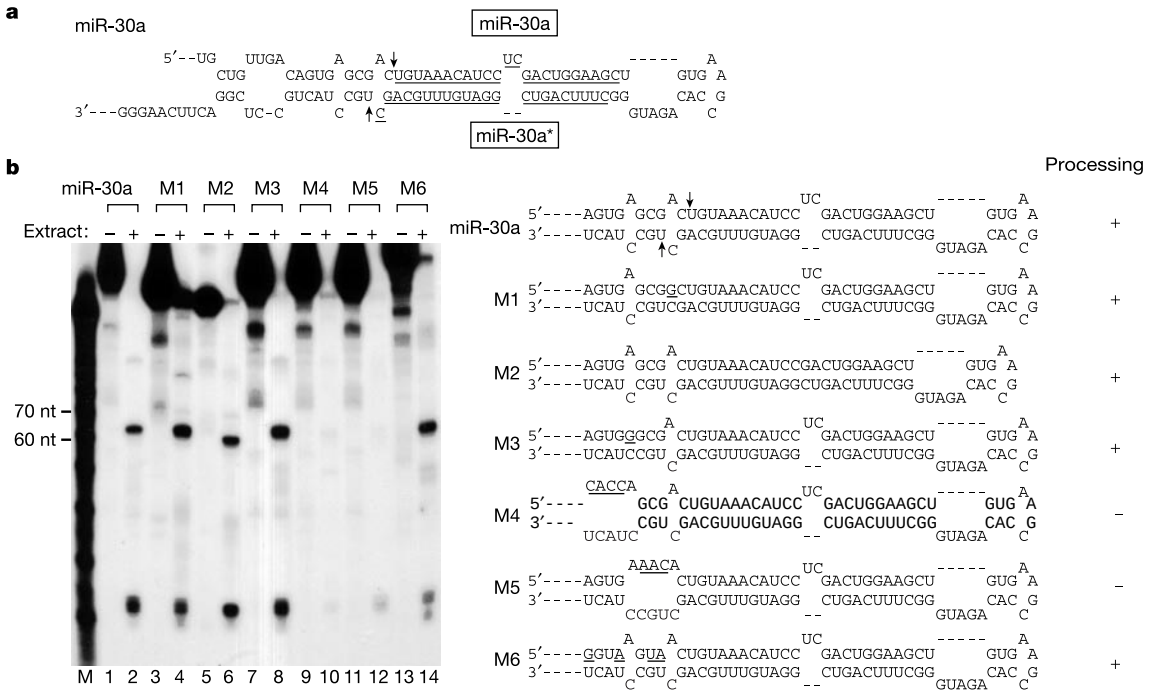

Figure 1 Cleavage sites and *cis*-acting requirements for the initiation step of miRNA processing. **a**, Sequences of the miR-30a precursor that are sufficient to support processing *in vitro*. The cleavage sites (the 5′ and 3′ ends of pre-miR-30a) are indicated by arrows. The sequences for mature miR-30a and miR-30a* are underlined. **b**, Site-directed mutagenesis of pre-miR-30a. Altered sequences are underlined. Note that all of the precursors contain the sequences covering 20 nt upstream and 25 nt downstream from the cleavage sites, as in **a**. Size markers (Decade marker, Ambion) were loaded on lane M.

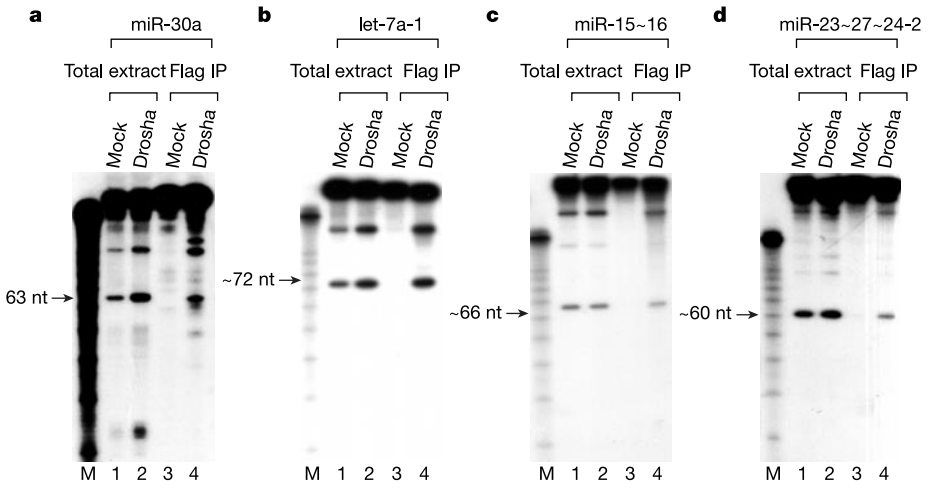

Figure 2 *In vitro* processing of miRNA by Drosha. Total-cell extract (Total extract) or immunoprecipitate (Flag IP) from mock-transfected (Mock) or Drosha–Flag-transfected HEK 293T cells (Drosha) were used for *in vitro* processing. **a**, miR-30a. **b**, let-7a-1. **c**, miR-15~16. **d**, miR-23~27~24-2.

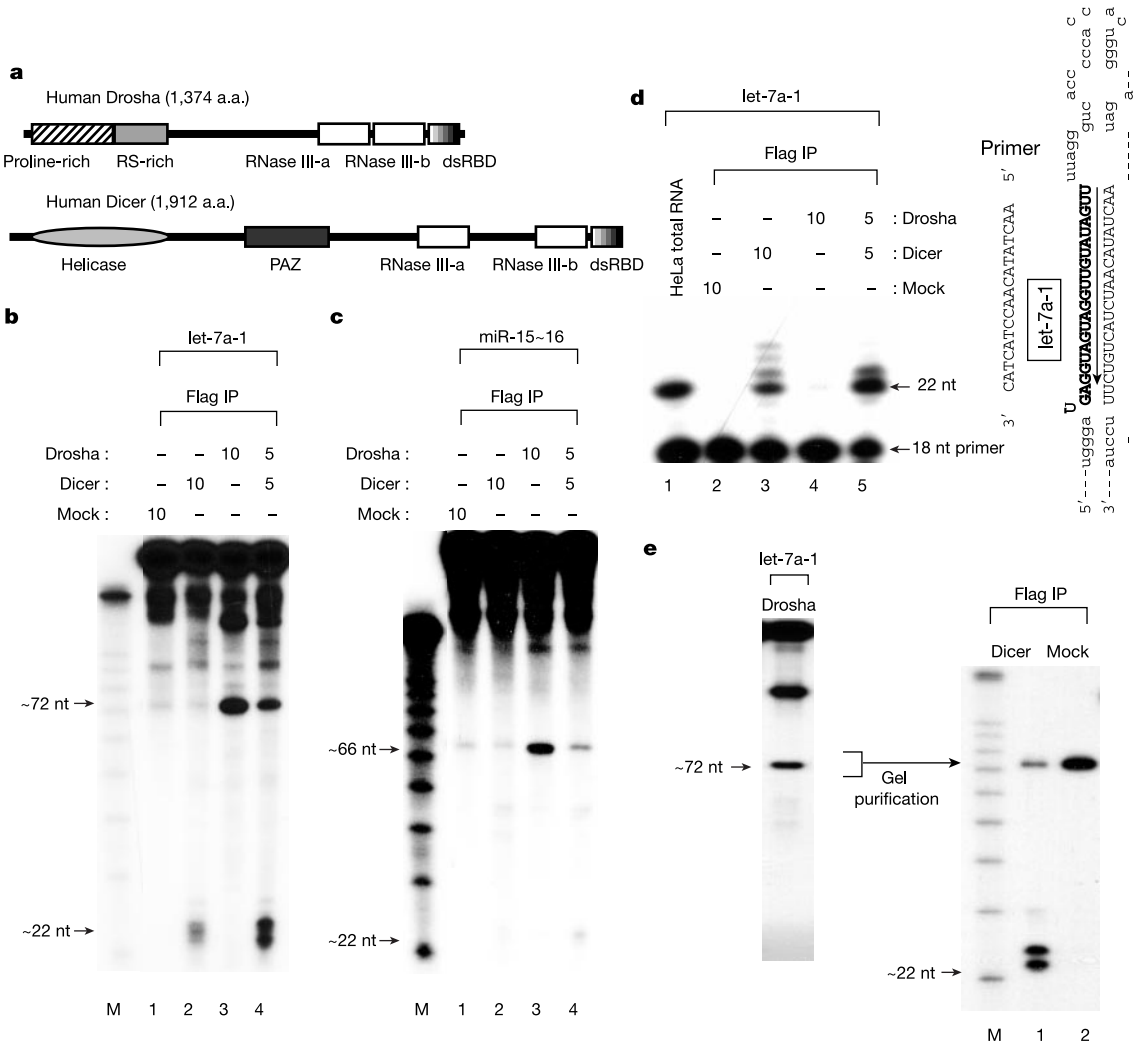

Figure 3 *In vitro* processing activities of Drosha and Dicer. **a**, Domain organization of Drosha and Dicer. **b**, *In vitro* processing of let-7a-1 using immunopurified Drosha and Dicer proteins. Indicated amounts of beads containing immunoprecipitated proteins (μl) were used for *in vitro* processing. **c**, *In vitro* processing of miR-15~16. **d**, Primer extension analysis using the HeLa total RNAs and the *in vitro* processing product. **e**, Stepwise processing of let-7a-1 by Drosha and Dicer. The indicated fragment from the *in vitro* processing using Drosha was gel-purified and incubated with Dicer.

carried out to remove the internal loops and bulges at or near the cleavage sites (M1, M2 and M3 in Fig. 1b). These mutants were processed efficiently, indicating that the internal loops (M1 and M3) and the bulge (M2) are not essential for processing. On the contrary, mutations that disturbed the stem structure (M4 and M5) markedly reduced the efficiency of the initial processing, whereas a mutant with altered sequences that retained the double-stranded (ds) structure (M6) made a good substrate for processing. This is consistent with a recent study in which the *cis*-acting element of miR-30a was mapped to the first stem outside the cleavage sites[20]. These results demonstrate the requirement for dsRNA structure around the cleavage sites, supporting the notion that the nuclease of interest may belong to the RNase III family. Members of the RNase III family are known to require divalent cations, including Mg^{2+}, for catalysis. It is noted that $MgCl_2$ was needed for the initial processing of miRNAs *in vitro* (data not shown).

RNase III proteins are dsRNA-specific endonucleases that introduce staggered cuts on each side of the RNA helix[22]. They are grouped into three classes on the basis of domain organization. Class I enzymes found in bacteria and yeasts contain one conserved RNase III domain and an adjacent dsRNA-binding domain (dsRBD). Class II enzymes, including Drosha and its homologues, have tandem RNase III domains and one dsRBD, as well as an extended amino-terminal domain of unknown function[23,24]. Dicer homologues in diverse species are members of class III and contain a putative helicase domain and a PAZ domain, in addition to tandem nuclease domains and a dsRBD. Human database searches revealed three RNase-III-type proteins. L44 contains a single RNase III domain and is a component of the large subunit of the mitochondrial ribosome[25]. The second RNase III, Dicer, is a cytoplasmic (endoplasmic reticulum–cytosol interface) protein[26,27] whose function is well established in the late stage of miRNA processing[15–19]. The third RNase III, Drosha, previously implicated in pre-rRNA (ribosomal RNA) processing, localizes predominantly to the nucleus[28], making it a good candidate for the nuclear processing factor for miRNAs.

To examine this possibility, Drosha protein tagged with the Flag epitope was expressed by transfection into HEK 293T cells and isolated by immunoprecipitation from the total-cell lysate using antibody-conjugated agarose. The precipitated protein was then used in an *in vitro* processing reaction. Treatment of the primary precursors with Drosha immunoprecipitate yielded fragments of 60–70 nt in length (Fig. 2), which corresponds to pre-miRNAs[14]. Therefore, Drosha can catalyse the initiation step of miRNA processing *in vitro*.

To analyse the processing activities of the two RNase-III-type proteins, Drosha and Dicer proteins were prepared by immunoprecipitation and used for *in vitro* processing. Drosha produced ~70-nt fragments, whereas Dicer cleaved the input RNA to ~22-nt fragments (Fig. 3b, c), showing that the two enzymes have different substrate specificity and mechanisms of action. To confirm the identity of the ~22-nt fragments, primer-extension analysis was carried out (Fig. 3d). Extension products of ~22 nt were detected from the *in vitro* processed products (Fig. 3d, lanes 3 and 5) as well as from HeLa total RNA (Fig. 3d, lane 1), verifying that the ~22-nt fragments included the authentic mature let-7a-1. Intriguingly, the final products appear to be more homogeneous with a combination of Drosha and Dicer (Fig. 3d lane 5) than with Dicer alone (lane 3), indicating that processing mediated by two enzymes may increase its accuracy. It is also interesting that a combination of Drosha and Dicer resulted in a higher yield of the final product of ~22 nt than when twice the amount of Dicer alone was applied (Fig. 3b–d). Thus, Drosha and Dicer may work together in a synergistic manner to increase the production of miRNA. Drosha and Dicer were not co-immunoprecipitated (data not shown), arguing against the possibility that they form a heterodimer to function coordinately. To determine whether Drosha acts upstream of Dicer, the Drosha product was gel-purified and used for a further round of *in vitro* processing using Dicer (Fig. 3e). The ~72-nt Drosha product from pri-let-7a-1 was processed to generate the ~22-nt fragments in the presence of Dicer. Therefore, processing can occur in a stepwise manner *in vitro*. Our data suggest that Drosha may generate optimal substrates for Dicer, and that stepwise processing may have certain advantages over Dicer by only operating in terms of accuracy and efficiency. Stepwise processing is likely to be prevalent *in vivo* owing to the separate localization of the two enzymes: Drosha localizes mainly to the nucleus[28], and Dicer is found mainly in the cytoplasmic compartment[26,27]. Consistent with the previous report[28], Drosha was immunoprecipitated mainly from the nuclear fraction, and nuclear Drosha catalysed the initiation step of processing *in vitro* (Supplementary Information). Thus, maturation of miRNA may be carried out consecutively by two RNase III proteins, first by Drosha in the nucleus, and later by Dicer in the cytoplasm (for a model, see Supplementary Information).

To confirm the role of Drosha in miRNA maturation, we carried out RNA interference (RNAi) to deplete Drosha in cultured cells, and examined the effect on endogenous miRNA biogenesis. Out of four different short interfering RNA (siRNA) duplexes designed to

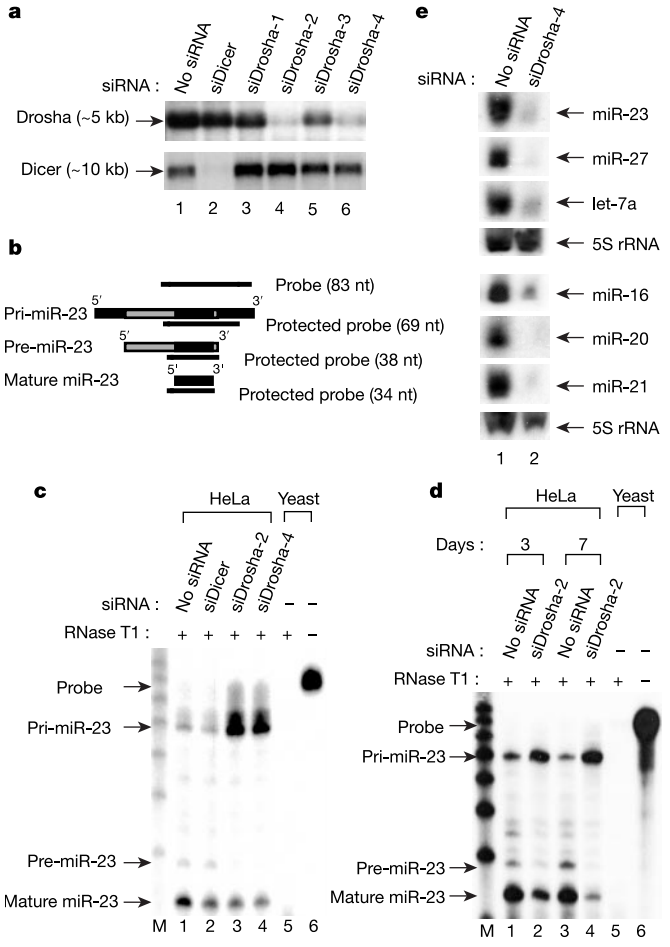

Figure 4 *In vivo* function of Drosha. **a**, Northern blot analysis of Drosha and Dicer messenger RNA, following RNAi in HeLa cells for three days. **b**, RNase protection assay. Three miRNA species, probe and protected fragments are presented schematically. **c**, One-hundred micrograms of total RNA from siRNA transfected HeLa cells were used for RPA. The cells were incubated for three days after transfection. **d**, After incubation for three or seven days after siRNA transfection, total RNA was prepared and 45 μg of total RNA was used for RPA. For the seven-day incubation, the cells were transfected twice. **d**, Northern blot analysis. Total RNA was prepared after double transfection and incubation for seven days. As a loading control, the blots were re-probed for 5S rRNA.

combat Drosha, two duplexes efficiently reduced the level of Drosha mRNA as shown by northern blot analysis (Fig. 4a). A control siRNA duplex targeting Dicer[15] also resulted in effective degradation of Dicer mRNA. Three days after siRNA transfection, an RNase protection assay (RPA) was performed to measure the steady-state level of three miRNA species: pri-, pre- and mature miRNA (Fig. 4b, c). From HeLa total RNA, three specific bands were detected that represented pri-miR-23, pre-miR-23 and mature miR-23. When Drosha was depleted, pri-miR-23 strongly accumulated whereas pre-miR-23 was diminished (Fig. 4c, lanes 3 and 4). We conclude that Drosha is required for the processing of pri-miR-23 into pre-miR-23. The knockdown of Dicer caused a reduction in mature miR-23, as expected (Fig. 4c, lane 2), but pre-miR-23 did not accumulate significantly under our experimental conditions, possibly because pre-miR-23 is unstable.

Mature miR-23 was reduced after Drosha knockdown, as expected (Fig. 4c), and it was further diminished after double transfection of siRNA and prolonged incubation for seven days (Fig. 4d). To show that our observations are not restricted to a certain RNA substrate, we performed northern blot analysis on six randomly chosen miRNAs: miR-23, miR-27, let-7a-1, miR-16, miR-20 and miR-21 (Fig. 4e). miR-30a was not included because of the low abundance of endogenous miR-30a (data not shown), as previously reported[29]. All the tested miRNAs significantly decreased after Drosha RNAi, suggesting that Drosha may be widely used for the maturation of most, if not all, miRNAs. We observed only a mild growth defect in cells (about 10%) after seven days, indicating that, under our assay conditions, blockade of miRNA processing precedes overall cellular malfunction and death. Drosha has previously been suggested to function in rRNA processing, on the basis of the observation that the depletion of Drosha using antisense oligonucleotides correlated with the accumulation of 12S and 32S pre-rRNAs[28]. Although the accumulation of pre-rRNA was modest, and the reduction in the final product, 5.8S rRNA, was not evident[28], we do not exclude the possibility that Drosha may have dual functions in both rRNA and miRNA processing.

Our study introduces a new player in miRNA biogenesis. As Drosha homologues are found in *C. elegans*, *D. melanogaster*, mice and humans[23,24], the stepwise processing of miRNAs mediated by Drosha and Dicer is likely to be conserved, at least in animals. Stepwise processing might be beneficial in terms of efficiency and accuracy of processing (Fig. 3). In addition, stepwise processing and compartmentalization might allow the fine regulation of miRNA biogenesis at multiple steps. It would be of great interest to understand how, and by what, miRNA-processing enzymes are regulated. Our study also reveals interesting differences between class II and III RNase III proteins in their substrate specificities. It is an open question how Drosha and Dicer recognize their targets in a specific manner when the primary sequences of diverse miRNAs show no conserved elements. In view of this, it will be important to determine structures of miRNA precursors and RNase III proteins. Further studies of Drosha will help to elucidate the action mechanism of RNase III, and to unravel the mechanism of miRNA biogenesis, the novel family of developmental regulators. □

Methods

Immunoprecipitation and *in vitro* processing

Proteins were expressed in transfected HEK 293T cells. Forty-eight hours after transfection, total extract was prepared in Buffer D (20 mM HEPES-KOH, pH 7.9, 100 mM KCl, 0.2 mM EDTA, 0.5 mM DTT, 0.2 mM PMSF, 5% glycerol) by sonication followed by centrifugation. Total extract was used for immunoprecipitation in Buffer D using anti-Flag M2 affinity gel (Sigma). After washing, the beads were drained and used for *in vitro* processing[14]. Thirty microlitres of processing reaction contained 15 μl of whole-cell extract or the beads from immunoprecipitation, 6.4 mM $MgCl_2$, 1 unit μl^{-1} of RNase Inhibitor (TAKARA), and the labelled transcripts of 1×10^4–1×10^5 c.p.m. The reaction mixture was incubated at 37 °C for 90 min.

Primer-extension analysis

Cold let-7a-1 precursor was synthesized *in vitro* and incubated with protein immunoprecipitates at 37 °C for 90 min. After phenol extraction and ethanol precipitation, the RNA was used for hybridization to 5′-end-labelled primer at 37 °C for 40 min, and subsequently for extension using SUPERSCRIPT II (GibcoBRL) at 50 °C for 30 min. Forty-five micrograms of HeLa total RNA were used as a control. Primer sequences are 5′-aactatacaacctactac-3′.

RNA interference

siRNA duplexes, siDrosha-1, siDrosha-2, siDrosha-3 and siDrosha-4 (Dharmacon), were designed to anneal to Drosha mRNA in which the target sequences were 5′-AACCGAA GAUCACCAUCUCUG-3′, 5′-AACGAGUAGGCUUCGUGACUU-3′, 5′-AAUCGGACC UUCGACAUGCAA-3′ and 5′-AAGGACCAAGUAUUCAGCAAG-3′, respectively. A siRNA duplex for Dicer has previously been described[15]. siRNA duplexes were transfected into HeLa cells using Oligofectamine Reagent (Invitrogen)[30]. Total RNA was prepared three days after transfection and used for northern blot analysis or RPA[14]. For double transfection, cells were split again three days after the first transfection, transfected once more on the fourth day, and incubated for three more days. The cells were incubated for seven days in total from the time of the first transfection.

Received 4 May; accepted 25 July 2003; doi:10.1038/nature01957.

1. Lee, R. C., Feinbaum, R. L. & Ambros, V. The *C. elegans* heterochronic gene *lin-4* encodes small RNAs with antisense complementarity to *lin-14*. *Cell* **75,** 843–854 (1993).
2. Reinhart, B. J. *et al.* The 21-nucleotide *let-7* RNA regulates developmental timing in *Caenorhabditis elegans*. *Nature* **403,** 901–906 (2000).
3. Lagos-Quintana, M., Rauhut, R., Lendeckel, W. & Tuschl, T. Identification of novel genes coding for small expressed RNAs. *Science* **294,** 853–858 (2001).
4. Lau, N. C., Lim, L. P., Weinstein, E. G. & Bartel, D. P. An abundant class of tiny RNAs with probable regulatory roles in *Caenorhabditis elegans*. *Science* **294,** 858–862 (2001).
5. Lee, R. C. & Ambros, V. An extensive class of small RNAs in *Caenorhabditis elegans*. *Science* **294,** 862–864 (2001).
6. Mourelatos, Z. *et al.* miRNPs: a novel class of ribonucleoproteins containing numerous microRNAs. *Genes Dev.* **16,** 720–728 (2002).
7. Llave, C., Kasschau, K. D., Rector, M. A. & Carrington, J. C. Endogenous and silencing-associated small RNAs in plants. *Plant Cell* **14,** 1605–1619 (2002).
8. Reinhart, B. J., Weinstein, E. G., Rhoades, M. W., Bartel, B. & Bartel, D. P. MicroRNAs in plants. *Genes Dev.* **16,** 1616–1626 (2002).
9. Lagos-Quintana, M. *et al.* Identification of tissue-specific microRNAs from mouse. *Curr. Biol.* **12,** 735–739 (2002).
10. Park, W., Li, J., Song, R., Messing, J. & Chen, X. CARPEL FACTORY, a Dicer homolog, and HEN1, a novel protein, act in microRNA metabolism in *Arabidopsis thaliana*. *Curr. Biol.* **12,** 1484–1495 (2002).
11. Llave, C., Xie, Z., Kasschau, K. D. & Carrington, J. C. Cleavage of Scarecrow-like mRNA targets directed by a class of *Arabidopsis* miRNA. *Science* **297,** 2053–2056 (2002).
12. Tang, G., Reinhart, B. J., Bartel, D. P. & Zamore, P. D. A biochemical framework for RNA silencing in plants. *Genes Dev.* **17,** 49–63 (2003).
13. Brennecke, J., Hipfner, D. R., Stark, A., Russell, R. B. & Cohen, S. M. Bantam encodes a developmentally regulated microRNA that controls cell proliferation and regulates the proapoptotic gene *hid* in *Drosophila*. *Cell* **113,** 25–36 (2003).
14. Lee, Y., Jeon, K., Lee, J. T., Kim, S. & Kim, V. N. MicroRNA maturation: stepwise processing and subcellular localization. *EMBO J.* **21,** 4663–4670 (2002).
15. Hutvagner, G. *et al.* A cellular function for the RNA-interference enzyme Dicer in the maturation of the *let-7* small temporal RNA. *Science* **293,** 834–838 (2001).
16. Bernstein, E., Caudy, A. A., Hammond, S. M. & Hannon, G. J. Role for a bidentate ribonuclease in the initiation step of RNA interference. *Nature* **409,** 363–366 (2001).
17. Grishok, A. *et al.* Genes and mechanisms related to RNA interference regulate expression of the small temporal RNAs that control *C. elegans* developmental timing. *Cell* **106,** 23–34 (2001).
18. Ketting, R. F. *et al.* Dicer functions in RNA interference and in synthesis of small RNA involved in developmental timing in *C. elegans*. *Genes Dev.* **15,** 2654–2659 (2001).
19. Knight, S. W. & Bass, B. L. A role for the RNase III enzyme DCR-1 in RNA interference and germ line development in *Caenorhabditis elegans*. *Science* **293,** 2269–2271 (2001).
20. Zeng, Y. & Cullen, B. R. Sequence requirements for micro RNA processing and function in human cells. *RNA* **9,** 112–123 (2003).
21. Elbashir, S. M., Lendeckel, W. & Tuschl, T. RNA interference is mediated by 21- and 22-nucleotide RNAs. *Genes Dev.* **15,** 188–200 (2001).
22. Zamore, P. D. Thirty-three years later, a glimpse at the ribonuclease III active site. *Mol. Cell* **8,** 1158–1160 (2001).
23. Filippov, V., Solovyev, V., Filippova, M. & Gill, S. S. A novel type of RNase III family proteins in eukaryotes. *Gene* **245,** 213–221 (2000).
24. Fortin, K. R., Nicholson, R. H. & Nicholson, A. W. Mouse ribonuclease III. cDNA structure, expression analysis, and chromosomal location. *BMC Genomics* **3,** 26 (2002).
25. Koc, E. C. *et al.* The large subunit of the mammalian mitochondrial ribosome. Analysis of the complement of ribosomal proteins present. *J. Biol. Chem.* **276,** 43958–43969 (2001).
26. Billy, E., Brondani, V., Zhang, H., Muller, U. & Filipowicz, W. Specific interference with gene expression induced by long, double-stranded RNA in mouse embryonal teratocarcinoma cell lines. *Proc. Natl Acad. Sci. USA* **98,** 14428–14433 (2001).
27. Provost, P. *et al.* Ribonuclease activity and RNA binding of recombinant human Dicer. *EMBO J.* **21,** 5864–5874 (2002).
28. Wu, H., Xu, H., Miraglia, L. J. & Crooke, S. T. Human RNase III is a 160-kDa protein involved in preribosomal RNA processing. *J. Biol. Chem.* **275,** 36957–36965 (2000).
29. Zeng, Y., Wagner, E. J. & Cullen, B. R. Both natural and designed micro RNAs can inhibit the expression of cognate mRNAs when expressed in human cells. *Mol. Cell* **9,** 1327–1333 (2002).
30. Elbashir, S. M. *et al.* Duplexes of 21-nucleotide RNAs mediate RNA interference in cultured mammalian cells. *Nature* **411,** 494–498 (2001).

Supplementary Information accompanies the paper on **www.nature.com/nature**.

Acknowledgements We are grateful to members of our laboratory and to K. Mitrophanous, J. M. Park and H. E. Kim for their critical reading of this manuscript and for discussion. This work was supported by the Korea Research Foundation and the BK21 Research Fellowship from the Ministry of Education and Human Resources Development of Korea.

Competing interests statement The authors declare that they have no competing financial interests.

Correspondence and requests for materials should be addressed to V.N.K. (narrykim@snu.ac.kr).

A structural state of the myosin V motor without bound nucleotide

Pierre-Damien Coureux[1], Amber L. Wells[2], Julie Ménétrey[1], Christopher M. Yengo[2], Carl A. Morris[2], H. Lee Sweeney[2] & Anne Houdusse[1]

[1]*Structural Motility, Institut Curie CNRS, UMR144, 26 rue d'Ulm, 75248 Paris cedex 05, France*
[2]*Department of Physiology, University of Pennsylvania School of Medicine, 3700 Hamilton Walk, Philadelphia, Pennsylvania 19104-6085, USA*

The myosin superfamily of molecular motors use ATP hydrolysis and actin-activated product release to produce directed movement and force[1]. Although this is generally thought to involve movement of a mechanical lever arm attached to a motor core[1,2], the structural details of the rearrangement in myosin that drive the lever arm motion on actin attachment are unknown. Motivated by kinetic evidence that the processive unconventional myosin, myosin V, populates a unique state in the absence of nucleotide and actin, we obtained a 2.0 Å structure of a myosin V fragment. Here we reveal a conformation of myosin without bound nucleotide. The nucleotide-binding site has adopted new conformations of the nucleotide-binding elements that reduce the affinity for the nucleotide. The major cleft in the molecule has closed, and the lever arm has assumed a position consistent with that in an actomyosin rigor complex. These changes have been accomplished by relative movements of the subdomains of the molecule, and reveal elements of the structural communication between the actin-binding interface and nucleotide-binding site of myosin that underlie the mechanism of chemo-mechanical transduction.

Myosin V is a myosin motor that has a number of structural and kinetic features that allow it to act as a two-headed processive motor protein[3]. The most notable feature is its long tandem repeat of six calmodulin/light-chain-binding sites, which form a long 'lever arm' that allows myosin V to take multiple 36-nm steps along an actin filament without detachment (that is, processive movement)[3,4]. This allows the molecule to function as a vesicle transporter[5]. To achieve processive movement, the rates of key kinetic steps of myosin V are very different from myosin II, which results in each head spending most of its ATPase cycle strongly bound to actin[6].

The current view of how myosin couples ATP hydrolysis and actin binding to movement is known as the lever arm hypothesis[1,2]. In essence the proposed mechanism is that nucleotide binding, hydrolysis and product release are all coupled to small movements within the myosin motor core. These movements are amplified and transmitted by a region that has been termed the 'converter'[7,8] to a lever arm consisting of a light-chain-binding helix and associated light chains. The lever arm further amplifies the motions of the converter into large directed movements[7–9]. In the absence of actin, ATP hydrolysis occurs, but product release is slow, thus trapping the lever arm in a primed or pre-power-stroke position. Binding to actin causes release of products, movement of the lever arm, and force generation concomitant with formation of strong binding between myosin and actin (see Supplementary Fig. 1).

Although there is growing evidence for this general scheme[1], the proposed structural details of the motor domain changes are based entirely on high-resolution structures of myosin II in states that bind weakly to actin, and thus do not represent force-generating states[2]. Crystals with either vanadate or AlF_4 plus MgADP reveal a state (the 'transition' state) that probably mimics the pre-power-stroke state of myosin compatible with ATP hydrolysis, and before actin binding[7,10,11]. The 'near-rigor' state, which has been seen with MgADP, MgATP, ATP analogues or no nucleotide in the active site[12,13], has been proposed to reveal the position of the myosin lever arm at the end of the power stroke on release of MgADP (an actomyosin state known as rigor). However, it cannot truly represent such a state as there is considerable kinetic evidence that demonstrates that the near-rigor conformation of myosin II cannot bind strongly to actin without significant structural rearrangements[2,14]. Thus current crystal structures of myosin II offer no explanation of how actin-induced product release increases the affinity of myosin for actin, and how ATP dissociates the actin–myosin nucleotide-free (rigor) complex after release of phosphate and MgADP.

As previously noted[6] (see also Supplementary Fig. 2), in the absence of nucleotide an expressed truncated form (truncated after the first calmodulin-binding domain) of myosin V with a bound essential light chain (LC1-sa with the extended amino terminus removed[15]) binds rapidly to actin in a concentration-dependent manner, is not temperature dependent, and does not saturate over the actin concentrations examined. The rate of skeletal myosin II actin binding is highly temperature dependent and saturates at a moderate rate and actin concentration[16]. This indicates that in the absence of nucleotide and actin, myosin II—which mostly populates the near-rigor conformational state—is in a very different conformation from that in the rigor complex that forms after adding actin. On the other hand, the kinetics of myosin V binding appear to be diffusion limited[6], implying that myosin V in the absence of nucleotide and actin is in a state that is nearly equivalent to the rigor state formed on the addition of actin.

Crystals of this nucleotide-free myosin V construct diffracted to 2.0 Å. The refined structure is unlike that of any of the myosin structures to date. However, as compared to the near-rigor or pre-power-stroke structures, the lever arm is in a position that is similar to that of the near-rigor state (see Supplementary Fig. 3).

Figure 1a demonstrates that there have been movements of the previously defined[8] subdomains of the myosin motor that allow a different actin interface, closure of a major cleft (50-kDa cleft) in the molecule, and weakening of nucleotide binding. These subdomains of the motor, which have been proposed to move as units connected by flexible connectors or 'joints', are the N-terminal, upper 50-kDa and lower 50-kDa subdomains, and the converter (to which the lever arm is attached). This structure reveals new conformations of the previously defined connectors[8] (switch II, relay and SH1 helix) as well as revealing the importance of a fourth connector (previously termed the 'strut[17]'), which links the lower and upper 50-kDa subdomains near the actin interface. Precise interactions mediated by these connectors, that are different for each myosin state, allow stabilization of the unique subdomain positions in each state. In our new state, for the first time in any myosin structure, there is a significant movement (25° rotation) of the upper 50-kDa subdomain relative to the N-terminal subdomain. As discussed below, this movement is critical for both rearrangement of the nucleotide-binding pocket and closure of the internal cleft between the two 50-kDa subdomains.

On the basis of attempts to dock the initial and subsequent high-resolution structures of myosin II into lower-resolution cryo-